

November 11, 2019

Keywords or phrases:

Invasion, Metastasis, 3D, Tumor Spheroids, Extracellular Matrix, Imaging, Drug Development

Real-Time Live-Cell Analysis of 3D Tumor Spheroid Invasion

Miniver Oliver¹, Kalpana Patel¹, Sandra Perez¹, Nevine Holtz², Sanjana Udayashankar², Tim Dale¹

1. Sartorius, Hertfordshire, United Kingdom

2. Sartorius, Ann Arbor, United States

Introduction

Cell invasion, a hallmark of malignant cancers, plays a key role in tumor dissemination and metastasis and is responsible for cancer-related deaths^{1,2}. The ability of tumor cells to form a metastatic tumor primarily involves cell morphological reorganization and degradation of the surrounding extracellular matrix (ECM). Conventional *in vitro* invasion models, such as the filter based transwell invasion assay (2D) are widely used to assess tumor cell invasion. However, lack of comprehensive cell-ECM interactions may limit their physiological relevance. Three dimensional (3D) tumor invasion models, like the one described in this application note, potentially mimic more effectively key features of the metastatic phenotype. Understanding the mechanisms concerned in tumor cell invasion may lead to limiting tumor progression and consequently cancer patient mortality.

3D tumor invasion models in combination with automated image analysis technology would enable temporal high throughput analyses of tumor invasion. The Incucyte[®] Live-Cell Analysis System is a fully automated phase contrast, brightfield and fluorescence image acquisition and analysis platform that resides within a standard cell culture incubator for optimal cell viability and maintenance of physiological relevance. The instrument is designed to scan tissue culture plates and flasks repeatedly over pre-determined time intervals, enabling users to continuously monitor cultures and generate quantifiable, kinetic information. The Incucyte[®] Spheroid Analysis Software Module acts as a fast, flexible and powerful control hub for continuous live-cell analysis including image acquisition, processing, and data visualization.

Find out more: www.sartorius.com/incucyte

Assay Principle

This application note describes the use of the Incucyte® Live-Cell Analysis System and Incucyte® Single Spheroid Invasion Assay to study the invasive potential and capacity of malignant tumor cells. The enhanced depth of focus Brightfield (DF® Brightfield) image acquisition enables real-time kinetic imaging of 3D single spheroids embedded in an extracellular matrix (Matrigel®). This superior image acquisition results in Brightfield images with high contrast that can be readily masked using built-in Incucyte® integrated image analysis software. Whole spheroid

and invading cell areas are automatically plotted over time and deliver a wealth of information on spheroid formation and invasive properties. Thousands of images may be acquired, analyzed, and graphed, with the capability to run up to six 96-well plates in parallel for increased throughput. We describe validation methods and data demonstrating the ability to kinetically visualize and quantify invasive capabilities of a range of cell types and assess sensitivity to cell invasion modulating compounds.

Material and Methods

Quick Guide

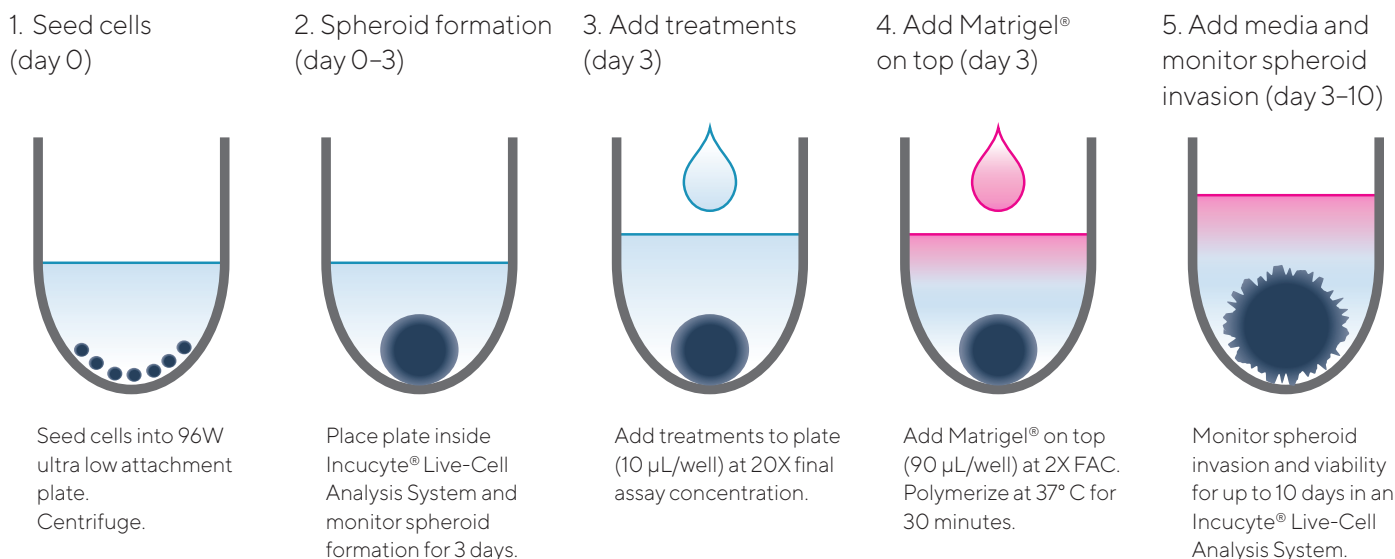


Figure 1: Assay Workflow

- Cells of interest are harvested, counted and plated into ULA round-bottom 96-well plates at desired densities (in 100 µL per well). Plates are centrifuged (125 g, 10 min, room temperature).
- Spheroid formation is monitored to desired size (e.g., 200–500 µm in diameter) with Brightfield and HD phase-contrast image acquisition (4X magnification) every 6 hours using Incucyte® Live-Cell Analysis System.
- Post spheroid formation compounds are added (10 µL at 20X final assay concentration (FAC) per well).
- Plate is placed on a pre-chilled CoolSink 96F within a CoolBox 96F box (~ 5 mins).
- Matrigel® is added on top (90 µL per well, at 2X FAC, e.g., 100% for 50% FAC) and polymerized at 37° C for 30 min.
- Media containing treatments at 1X FAC is added on top of polymerized Matrigel® (50 µL per well).
- Spheroid Invasion is monitored in Incucyte® Live-Cell Analysis System (6 hour repeat scanning, up to 2 weeks). Tumor size is reported in real-time based on Brightfield image analysis.

All cell culture reagents were obtained from Life Technologies unless otherwise noted. U87-MG (ATCC), A172 (ATCC) and HT1080 (ATCC) cells were cultured in F-12K medium supplemented with 10% FBS, 1% Pen | Strep plus 1% Glutamax and grown to confluence in 75 cm² tissue culture treated flasks. Cells were harvested and seeded into ULA 96-well plates (Corning #7007, SBio #MS-9096UZ, BRAND #781900) such that 3 days post cell seeding, spheroids formed with desired size. Spheroid formation was monitored in an Incucyte® over 3 days at 6 h intervals. Once formed, spheroids were embedded in Matrigel® (Corning #356234) at varying concentrations (2.25–4.5 mg/mL) to induce the spheroid invasion assay. All compounds were purchased from Tocris Bioscience.

Quantifying Single Spheroid Invasive Properties over Time

U87-MG spheroids formed for 3 days, were embedded in Matrigel® (4.5 mg/mL) in the presence and absence of actin polymerization inhibitor, Cytochalasin D (Cyto D) and DF-Brightfield (DF-BF) images acquired every 6 h.

In the presence of Matrigel®, U87-MG control spheroids rapidly increased in overall size (whole spheroid area) and exhibited marked invasive capabilities over time (7-fold increase in invading cell area), while Cyto D caused a marked inhibition of spheroid invasion (Figure 2, time-course plots).

Single spheroid invasive properties were measured using Incucyte® Spheroid Analysis Software Module, which tracks and quantifies changes in spheroid size (whole spheroid area or invading cell area) over time. Figure 2 illustrates the software's ability to accurately segment the whole spheroid area (yellow outline mask) and the invading cell area (blue outline mask) (Figure 2, images).

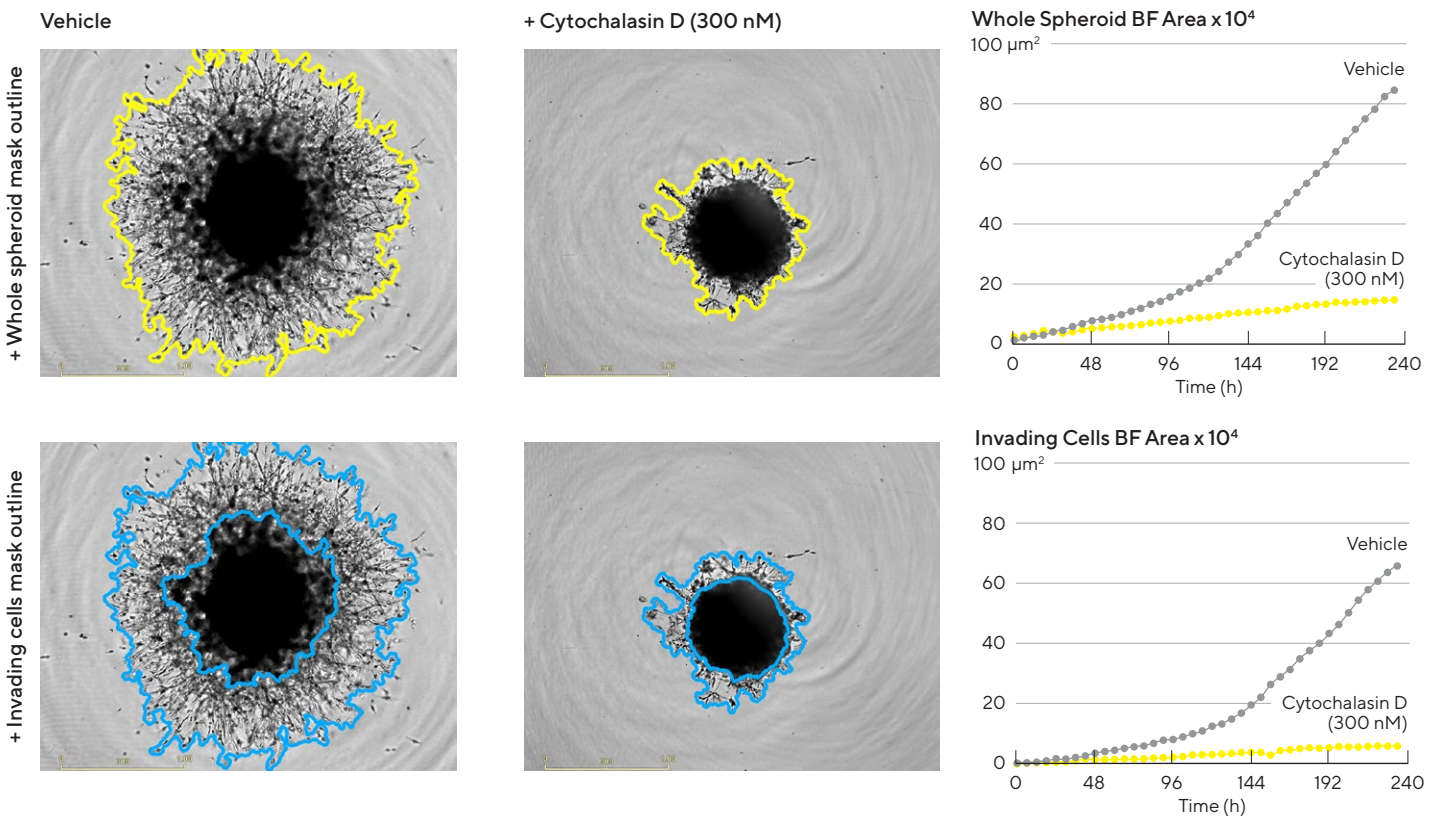


Figure 2: Quantification of single spheroid invasion using Incucyte® real-time analysis. U87-MG cells were seeded in a ULA round bottom 96-well plate (2,500 cells/well) and allowed to form spheroids for 3 days. Spheroids were subsequently treated with vehicle or Cytochalasin D (Cyto D) prior to embedding in Matrigel® (4.5 mg/mL). Incucyte® depth of focus brightfield (DF-BF) images (5 d post treatment) show effect of Cyto D on spheroid invasion (whole spheroid; yellow outline mask or invading cells; blue outline mask). Note extensive invasive phenotype of vehicle treated compared to Cyto D treated spheroids. Time-course plots show the individual well BF area (Whole Spheroid or Invading Cell BF Areas, μm^2) over time (h). Data were collected over a 240 h period at 6 h intervals. All images captured at 4X magnification. Each data point represents mean \pm SEM, n = 4 wells.

Cell Type Specific Spheroid Invasive Potential

To assess the metastatic potential of tumor cells in 3D, U87-MG (glioblastoma), A172 (glioblastoma) and HT1080 (fibrosarcoma) spheroids were formed for 72 h in ULA round bottom 96-well plates and subsequently embedded in Matrigel® (4.5 mg/mL). Changes in tumor spheroid invasive properties were kinetically monitored and quantified over time (7 d).

Invading cell area segmentation shown in blue (Figure 3, images), enabled kinetic quantification of spheroid metastatic potential and illustrates the ability of the Incucyte® Live-Cell Analysis System to accurately differentiate between the invading cell area and spheroid body area across a range of cell types. To account for variation in size following spheroid formation, the whole spheroid area was normalized to spheroid size at $t = 0$ h and automatically plotted over time.

Acquired DF-BF images and time-course plots revealed cell type specific invasive capabilities. U87-MG spheroids exhibited the greatest invasive potential. At 168 h, whole spheroid area of U87-MG spheroids (ratio: 32) increased to approximately 2X and 4X the size of HT1080 (ratio: 18) and A172 (ratio: 8) spheroids respectively (Figure 3, Whole Spheroid BF Area ratio time-course).

Though different in overall size, A172 and HT1080 spheroids showed comparable invasive potential over time (~10-fold at 168 h) (Figure 3, invading cell area time-course).

Differences in invasive potential shown across cell types may suggest distinct mechanisms of cell motility and invasive modalities¹. Additional experimentation is required to fully understand mechanisms underlying these differences.

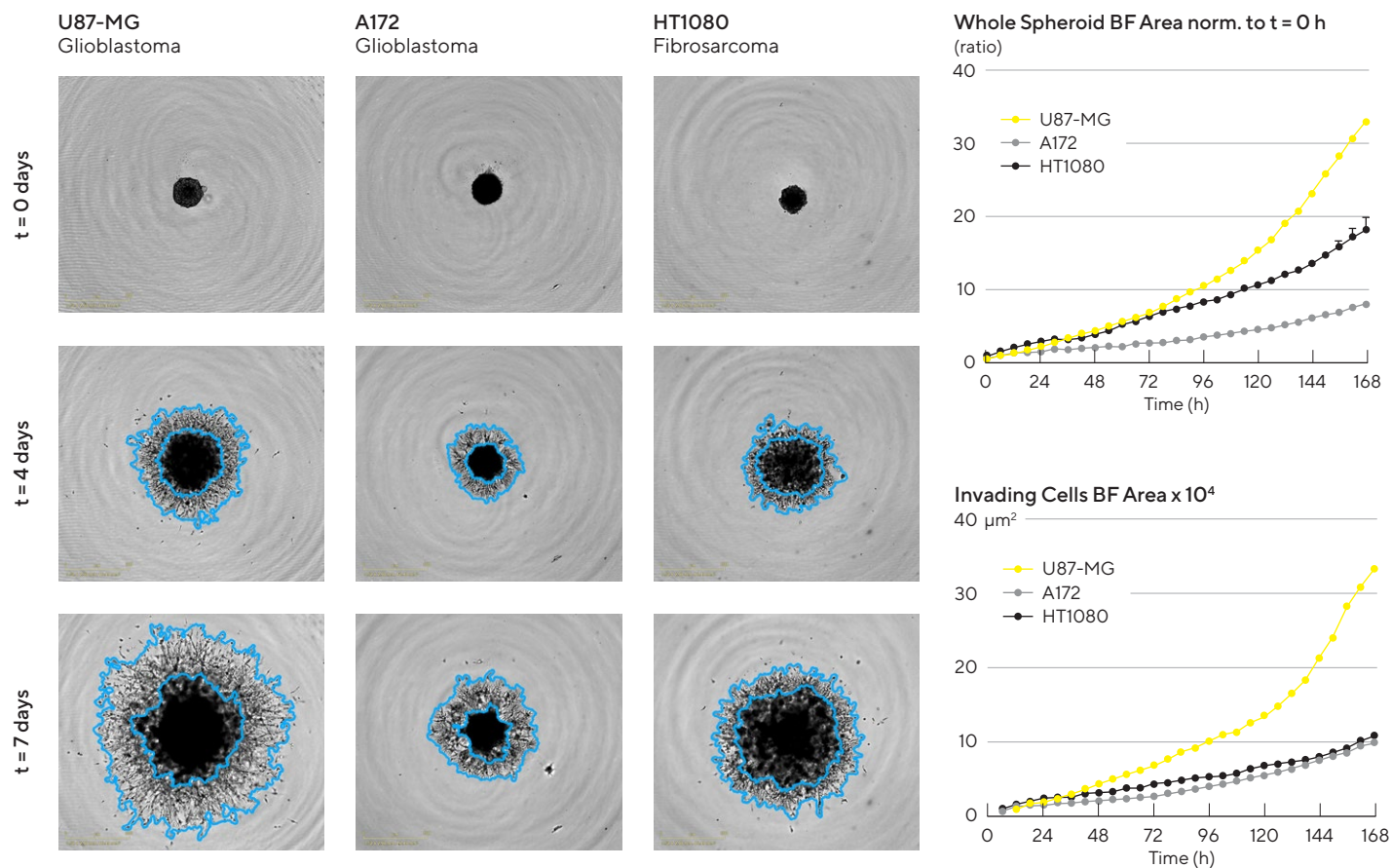


Figure 3: Assess cell type specific invasive capabilities over time. U87-MG, A172 and HT1080 cells were seeded in ULA round bottom 96-well plates (2,500 cells/well; U87-MG, HT1080 or 5,000 cells/well; A172) and allowed to form spheroids (3 d) prior to Matrigel® addition (4.5 mg/mL). Brightfield images and time-courses of spheroid area (Whole Spheroid BF Area normalized to $t = 0$ h or Invading Cell BF Area) show differences in invasive capacity across cell types. Invading cell area mask outline shown in blue, illustrates the extent of invasive capacity. Data were collected over 168 h at 6 h intervals. All images captured at 4X magnification. Each data point represents mean \pm SEM, $n = 4$ wells.

Impact of Matrigel® Concentration on Spheroid Invasive Capacity

Metastasis is a multistep process in which extracellular matrix (ECM) and cancer cell cytoskeleton interactions are pivotal in promoting the invasive potential of tumor cells². To understand the relationship between ECM properties (e.g., rigidity), invasive capacity and invasive phenotype, HT1080 spheroids formed for 72 h, were embedded in increasing concentrations of Matrigel® (1.13–4.5 mg/mL).

DF-BF images and quantification of whole spheroid area demonstrated that spheroid invasive capacity is Matrigel® concentration-dependent. (Figure 4A, B). Images also illustrate the effect of Matrigel® concentration on the density of spindle-like protrusions (invadopodia). Marked density and elongation of invadopodia is seen at the

highest concentration of Matrigel® (4.5 mg/mL) (Figure 4A, zoomed images).

Interestingly, a bell-shaped relationship of ECM concentration on spheroid invasion capacity was revealed in U87-MG and A172 spheroids with the greatest invading cell area attained at 2.25 mg/mL Matrigel® (Figure 4C). While an extension of the concentration range is required to confirm this observation, others have reported that at an optimal matrix concentration, cells at the periphery of the spheroid readily align with matrix fibers and rapidly invade the surrounding ECM. Whereas at higher concentrations, cell motility is reduced by the rigidity of the matrix³.

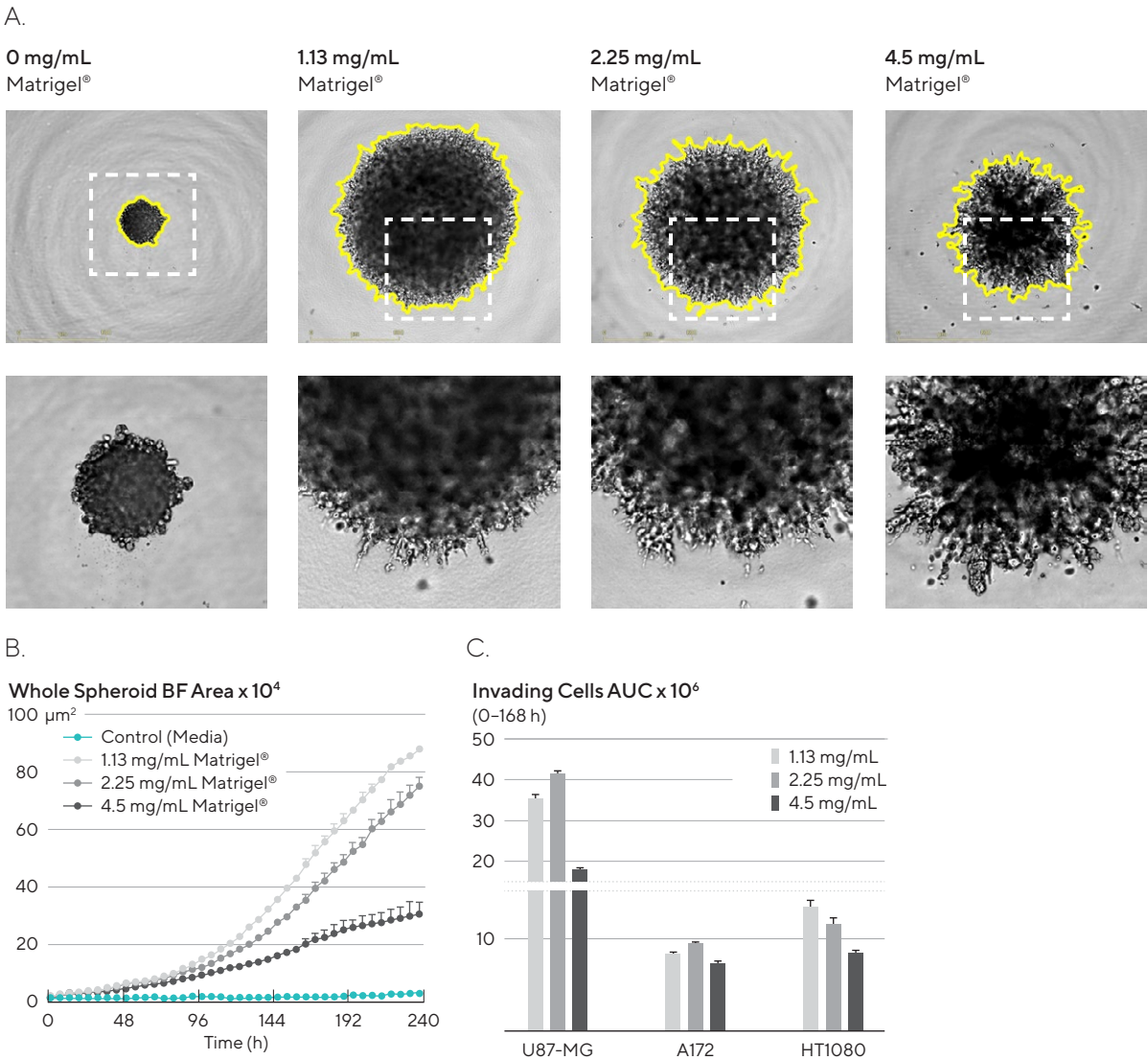
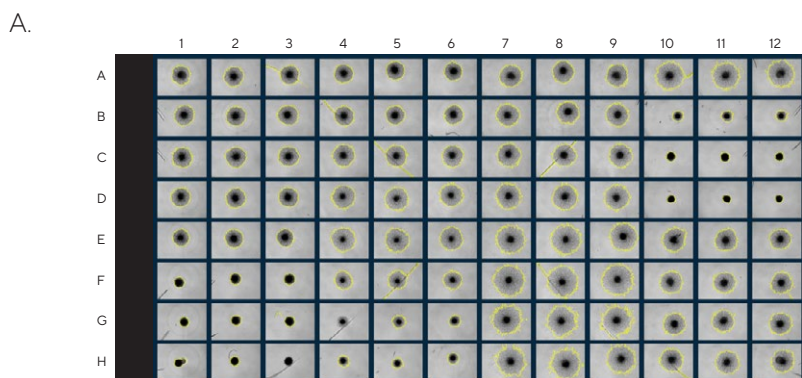


Figure 4: Effects of Matrigel® concentration on spheroid invasion. HT1080 cells were seeded in a ULA round bottom 96-well plate (2,500 cells/well) and allowed to form spheroids (3 d) prior to Matrigel® addition at varying concentrations (1.13 - 4.5 mg/mL). Brightfield images (7 d post Matrigel® addition) show effects of Matrigel® concentration on spheroid invasive capacity (A), whole spheroid area outline in yellow. Time-course shows individual well Whole Spheroid BF Area (μm²) over time (h) and dependency on Matrigel® concentration (B). Bar chart represents area under the curve (AUC) analysis of the Invading Cell BF Area time-course data (0-7 d, post Matrigel® addition) across multiple cell types (C). Data were collected over 240 h at 6 h intervals. All images captured at 4X magnification. Each data point represents mean ± SEM, n = 4 wells.

96-Well 3D Single Spheroid Invasion Assay for Pharmacological Analysis

To exemplify the amenability of this 3D tumor spheroid invasion assay to anti-metastatic compound testing, a pharmacological study was performed in U87-MG, A172 and HT1080 cells. Spheroids (formed 3D, in ULA round bottom 96-well plates) were treated with a range of invasion modulating compounds and subsequently embedded in Matrigel® (2.25 mg/mL or 4.5 mg/mL) to induce invasion (up to 10 d).

The Incucyte® real-time, automated Vessel Views and time-course Microplate Graph enabled rapid assessment of compound effects on spheroid invasion. Cyto D and PP242 caused a concentration dependent inhibition of U87-MG spheroid invasion, while little effect was observed by Blebbistatin (Figure 5 A, B).



B. Whole Spheroid BF Area (0-7 days)

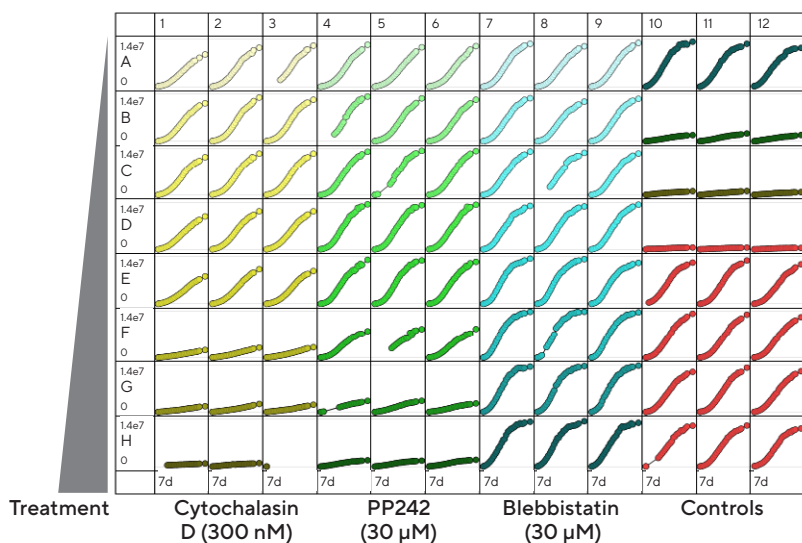


Figure 5: Rapid visualization and assessment of treatment effects using Incucyte® Vessel Views. U87-MG cells were seeded in ULA round bottom 96-well plates (2,500 cells/well) and allowed to form spheroids (3 d). Spheroids were then treated with serial dilutions of anti-metastatic compounds and embedded in Matrigel® (4.5 mg/mL) to induce invasion (up to 10 d). Incucyte® Microplate Graph show effects of treatments on spheroid invasion (Whole Spheroid BF Area; yellow outline mask) 5 d post treatment (A and B). Images captured at 4X magnification.

Elucidating Treatment Effects on Single Spheroid Invasion and Proliferation

The validity of 3D *in vitro* spheroid invasion models to assess the metastatic effects of treatments, relies on their ability to distinguish effects on spheroid invasion and spheroid proliferation. Being able to discriminate between the area covered by cells within the spheroid body from that covered by the invading cell region (invadopodia) is key. Here we illustrate how this spheroid invasion application and associated quantification and analysis approaches is able to address this.

A panel of known anti-metastatic compounds were tested for their effects on U87-MG spheroid invasion. Representative DF-BF images revealed a wide range of inhibitory effects on spheroid invasion (Figure 6A). With the exception of Blebbistatin, which appeared pro-invasive, all compounds inhibited spheroid invasion as reported by a reduction in both whole spheroid and invading cell areas (Figure 6B, light and dark grey bars respectively). While comparable attenuation of spheroid size was observed with both Cyto D (90% at 300 nM) and PP242 (80% at 30 μM), a striking and marked inhibition of the invading

cell area (invadopodia) was only evident with Cyto D (Figure 6A, size of blue mask, Figure 6B dark gray bars).

Normalization of the invading cell area to the whole spheroid area revealed that although similar in overall size 96 h post treatment, 80% (PP242) and 30% (Cyto D) of the total spheroid size was attributed to the invading cell region (Figure 6C). Performing a simple subtraction of the invading cell area from the whole spheroid area, provides a measure for the size of the spheroid body and hence, a measure for spheroid proliferation in this model of spheroid invasion. The reduced size of PP242 treated spheroids and the comparable sizes of both Cyto D and vehicle (in the

absence of Matrigel®) treated spheroids, further supports the anti-proliferative rather than anti-invasive properties of PP242 (Figure 6D).

To validate this analysis approach, a separate study conducted in the absence of Matrigel® permitted assessment of compound effects on spheroid proliferation alone. After formation, U87-MG spheroids were treated with compounds (96 h). Effects on spheroid growth and changes in spheroid size (Largest Object BF Area metric) were quantified using the Incucyte®. Figure 6E further supports and shows the inhibitory effects of PP242 (30 µM) but not Cyto D (300 nM) on spheroid growth.

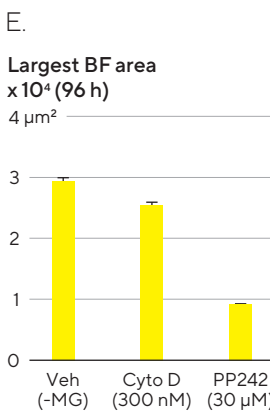
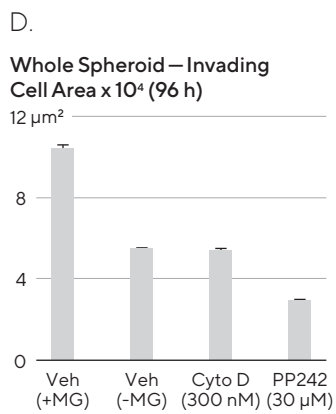
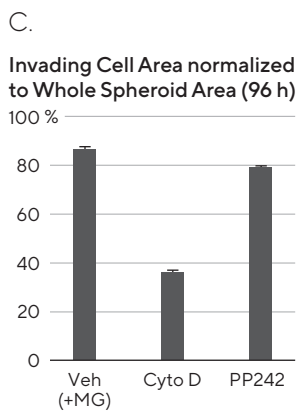
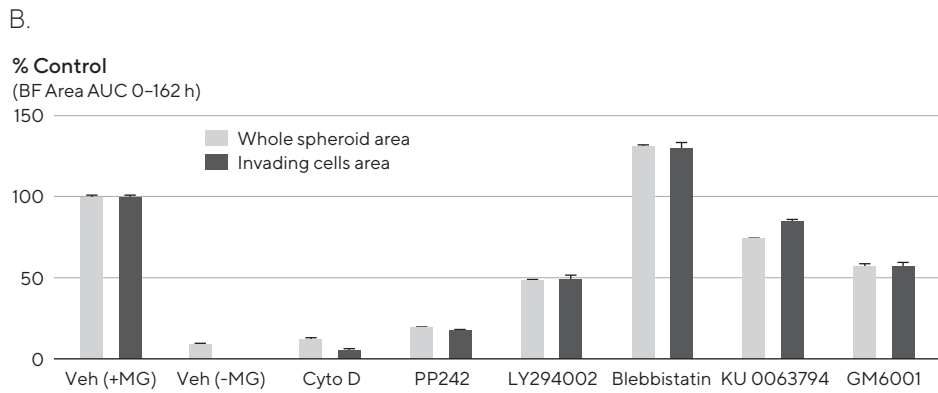
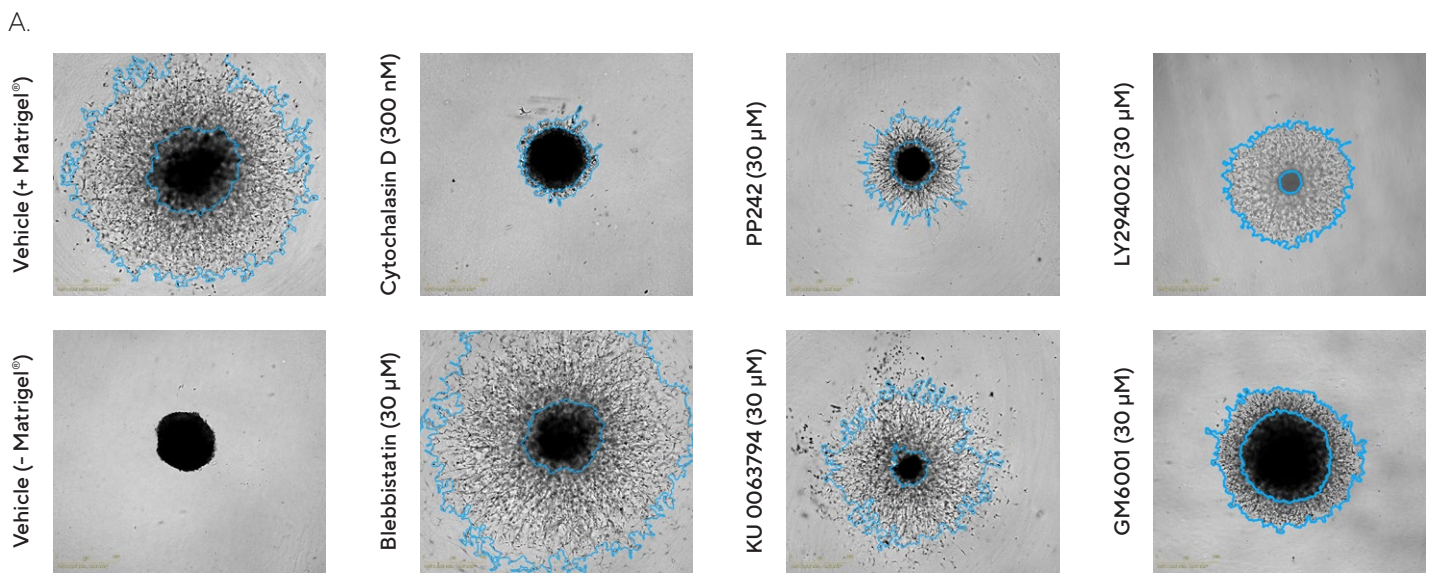


Figure 6: Effect of cell signalling inhibitors on spheroid invasion. U87-MG cells were seeded in a ULA round bottom 96-well plate (2,500 cells/well) and allowed to form spheroids (3 d) prior to treatment with a range of known inhibitors and embedded in Matrigel® (4.5 mg/mL). Incucyte® BF images (A) (4 d post treatment) show treatment effects on spheroid invasion. Bar chart (B) represents the area under the curve (AUC) analysis of the Whole Spheroid and Invading Cell BF Area (µm²) time-course data (0–162 h, post treatment). Note the inhibitory and stimulatory effects on invasion caused by Cytochalasin D (Cyto D) and Blebbistatin respectively. Data normalization (96 h post treatment) show effect of Cyto D and PP242 on invading cell regions (C). Subtraction of invading cell area from whole spheroid area (D). A separate but identical study performed in the absence of Matrigel® shows size (BF area) of spheroids 96 h post treatment with Cyto D and PP242 (D). Data were collected over a 162 h period at 6 h intervals. All images captured at 4X magnification. Each data point represents mean ± SEM, n = 3.

Cell Type Specific Pharmacology

The pharmacology of anti-metastatic compounds was assessed across multiple cell types. Concentration response curves (CRCs) representing the area under the curve analysis of time-course data were generated (invading cells area, 0–168 h) for Cyto D (actin polymerization inhibitor), PP242 (dual mTORC1/2 inhibitor) and GM6001 (MMP inhibitor) (Figure 7).

Cytochalasin D, was a strong inhibitor of invasion returning equipotent values for inhibition across all cell types (IC_{50} 30 nM for U87-MG, 30 nM for A172, 28 nM for HT1080). Concentration dependent inhibition of invasion was also observed with PP242 across all cell types (IC_{50} 0.88 μ M for A172, 3.2 μ M for HT1080, 5 μ M for U87-MG). However, this inhibition was incomplete and partial in U87-MG spheroids (~ 60% at 30 μ M). GM6001 appeared only to cause inhibition of HT1080 spheroid invasion (IC_{50} 6.3 μ M) with modest inhibitory effects on the other cell types.

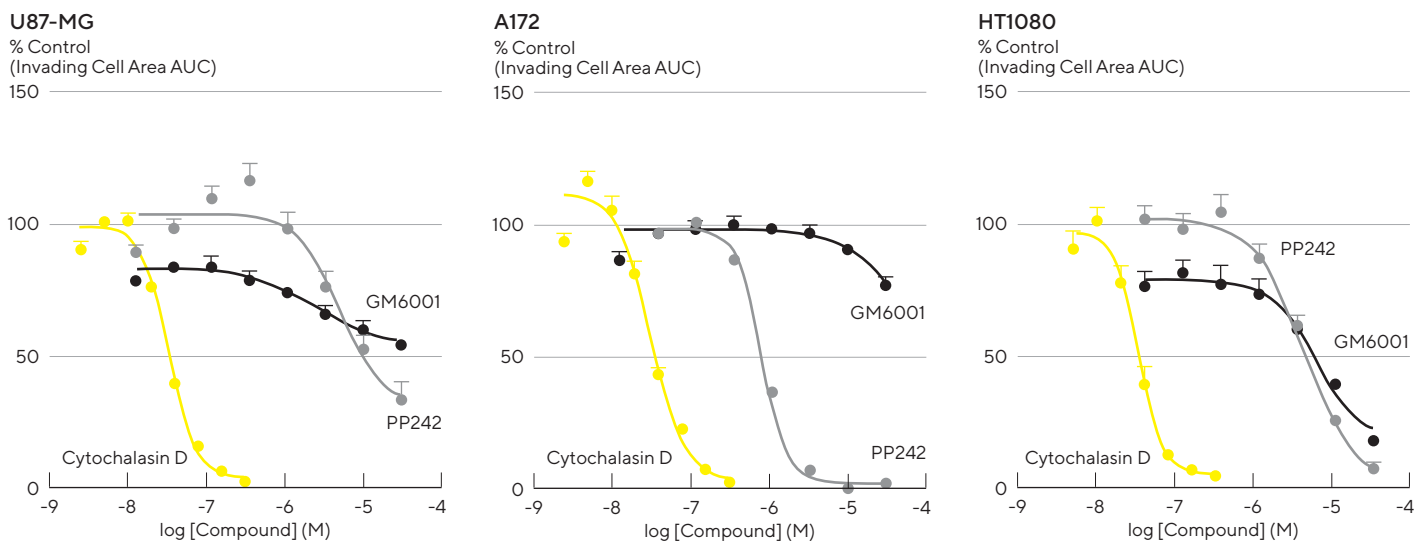


Figure 7: Distinguish pharmacological profiles of anti-metastatic compounds through concentration response curve generation. U87-MG, A172 and HT1080 cells were seeded in ULA round bottom 96-well plates (2,500 cells/well; U87-MG, HT1080 and 5,000 cells/well; A172) and allowed to form spheroids (3 d) prior to treatment. Spheroids were subsequently embedded in 2.25 mg/mL Matrigel® and spheroid invasion was monitored for 10 d. Representative concentration response curves (CRCs) of the area under the curve (AUC) analysis of the invading cell area (μ m²) (0–7 d). Data were collected over a 240 h period at 6 h intervals. Each data point represents mean \pm SEM, n = 3 separate test occasions.

Conclusions

In this application note, we demonstrate the use of the Incucyte® Live-Cell Analysis System, in combination with the Incucyte® Spheroid Analysis Software Module, to facilitate kinetic acquisition and quantification of 3D single spheroid invasion. We have shown:

- The capability to kinetically visualize and quantify tumor spheroid invasion properties
- Live-cell imaging and analysis revealed cell type specific temporal invasive potential
- Live-cell imaging and analysis demonstrate Matrigel® concentration-dependent effects on spheroid invasion capacity
- Available metrics and analysis approaches permit effects on spheroid invasion and spheroid proliferation to be probed
- The utility of our 3D tumor invasion model for real-time compound profiling in a 96-well format to identify and distinguish new or existing compounds effects on tumor invasion

The Incucyte®'s Single Spheroid Invasion Assay, in combination with fully integrated imaging and analysis solutions, enable both reproducible and high throughput analyses of tumor invasion. With no need for selection of a predefined end-point, consistent segmentation and quantification of brightfield images enable kinetic assessment of single spheroid invasive properties and effects of anti-metastatic agents.

The Incucyte® automated image acquisition, combined with user-friendly analysis tools and lab tested protocols, allows non-expert users to quickly generate reproducible data, perform analysis, and generate publication ready graphics. Taken together, the Incucyte® Live-Cell Analysis System, Spheroid Analysis Software Module and reagents provide a unique and efficient technical platform that can be incorporated into existing workflows.

References

1. Oraiopoulou, *et al.* **Integrating *in vitro* experiments with *in silico* approaches for Glioblastoma invasion: the role of cell-to-cell adhesion heterogeneity.** *Nature: Scientific Reports*, 8;16200 (2018)
2. Goertzen, *et al.* **Three-Dimensional quantification of spheroid degradation-dependent invasion and invadopodia formation.** *Biol Proceed Online*, 20;20 (2018)
3. Ahmadzadeh, *et al.* **Modeling the two-way feedback between contractility and matrix realignment reveals a nonlinear mode of cancer cell invasion.** *PNAS*, 114(9);E1617-E1626 (2017)

Sales and Service Contacts

For further contacts, visit
www.sartorius.com

Essen BioScience, A Sartorius Company

www.sartorius.com/incucyte

E-Mail: AskAScientist@sartorius.com



North America

Essen BioScience Inc.
300 West Morgan Road
Ann Arbor, Michigan, 48108
USA
Telephone +1 734 769 1600
E-Mail: orders.US07@sartorius.com

APAC

Essen BioScience K.K.
4th Floor Daiwa Shinagawa North
Bldg.
1-8-11 Kita-Shinagawa
Shinagawa-ku, Tokyo
140-0001
Japan
Telephone: +81 3 6478 5202
E-Mail: orders.US07@sartorius.com

Europe

Essen BioScience Ltd.
Units 2 & 3 The Quadrant
Newark Close
Royston Hertfordshire
SG8 5HL
United Kingdom
Telephone +44 1763 227400
E-Mail:
euorders.UK03@sartorius.com

Specifications subject to change without notice.

© 2020. All rights reserved. Incucyte, Essen BioScience, and all names of Essen BioScience products are registered trademarks and the property of Essen BioScience unless otherwise specified. Essen BioScience is a Sartorius Company.

Publication No.: 8000-0719-B00 Status: 08 | 2020